

# Third Order Density Perturbation and One-loop Power Spectrum in a Dark Energy Dominated Universe

Ryuichi Takahashi

*Department of Physics and Astrophysics, Nagoya University, Chikusa, Nagoya  
464-8602, Japan*

We investigate the third-order density perturbation and the one-loop correction to the linear power spectrum in the dark energy cosmological model. Our main interest is to understand the dark energy effect on the baryon acoustic oscillation in quasi-nonlinear regime ( $k \approx 0.1h/\text{Mpc}$ ). Analytical solutions and simple fitting formulae are presented for the dark energy model with the general time varying equation of state  $w(a)$ . It turns out that the power spectrum coincides with the approximate result based on the EdS (Einstein de-Sitter) model within 1% for  $k < 0.4h/\text{Mpc}$  at  $z = 0$  in the WMAP 5yr best-fitting cosmological model, which suggests that the cosmological dependence is very small.

## §1. Introduction

Revealing the nature of dark energy is fundamentally important not only for astrophysics but also for particle physics. Constraints on the dark energy from astronomical observations is very influential for them. Baryon acoustic oscillations (BAO) in the galaxy power spectrum provide the strong constraint on the dark energy by using its acoustic scale as a standard ruler. The large galaxy surveys such as Sloan Digital Sky Survey and two degree field already provide the constraint and the future larger surveys are currently planned to detect it more accurately.<sup>1)–4)</sup> Hence the accurate theoretical model of the BAO is crucial, and many authors have been investigating by the numerical simulations<sup>5)–11)</sup> and by the perturbation theory (including the renormalized perturbation theory).<sup>13)–21)</sup>

Previously several authors investigated the third-order density perturbation and derived the one-loop correction to the linear power spectrum in the EdS model.<sup>23)–28)</sup> Similarly for the cosmological constant model, Bernardeau (1994) presented the third-order perturbation solution (see also references 32)–36)). They found that the dependence of the cosmological model on the second- and third-order perturbations is very small, if the scale factor in the EdS model is replaced by the linear growth factor.<sup>\*</sup>) However, since the theoretical model of the BAO should archive the sub percent accuracy to provide a strong constraint on the dark energy, it is useful to re-investigate this topic to check the accurately of the above assumption. In this short paper, we calculate the third-order density perturbation, newly including the dark energy with the time varying equation of state, and derive the one-loop power spectrum analytically for the first time. We compare our results with the approximate results based on the EdS model in detail, and discuss the influence on the

---

<sup>\*</sup>) Martel & Freudling (1991) and Scoccimarro et al. (1998) showed that this assumption is valid if  $f \equiv d \ln D_1 / d \ln a = \Omega_M^{1/2}$ . However, since  $f \approx \Omega_M^{0.6}$ , the approximation is not accurate.

power spectrum near the baryon acoustic scale.

Throughout this paper, we use  $\delta$  as the density fluctuation,  $\theta (= \nabla \cdot \mathbf{v})$  as the divergence of the peculiar velocity field, and  $\tau = a(t)dt$  as the conformal time,  $\Omega_M$ ,  $\Omega_K$  and  $\Omega_X$  are the density parameter for the matter, the curvature and the dark energy at present, and  $w(a)$  is the equation of state of dark energy. The Hubble expansion rate is  $H^2(a) = H_0^2 \left[ \Omega_M a^{-3} + \Omega_K a^{-2} + \Omega_X \exp \left[ 3 \int_a^1 da' (1 + w(a')) / a' \right] \right]$ .

## §2. Basics

The equation of motion determines the growth of the density field  $\delta(\mathbf{k}, \tau)$  and velocity field  $\theta(\mathbf{k}, \tau) (\equiv i\mathbf{k} \cdot \mathbf{v}(\mathbf{k}, \tau))$  in the Fourier space is<sup>31)</sup>

$$\frac{\partial \delta(\mathbf{k}, \tau)}{\partial \tau} + \theta(\mathbf{k}, \tau) = - \int d^3 \mathbf{q} \alpha(\mathbf{q}, \mathbf{k} - \mathbf{q}) \theta(\mathbf{q}, \tau) \delta(\mathbf{k} - \mathbf{q}, \tau), \quad (2.1)$$

$$\begin{aligned} \frac{\partial \theta(\mathbf{k}, \tau)}{\partial \tau} + a(\tau) H(\tau) \theta(\mathbf{k}, \tau) + \frac{3}{2} a^2(\tau) \Omega_M(\tau) H^2(\tau) \delta(\mathbf{k}, \tau) \\ = - \int d^3 \mathbf{q} \beta(\mathbf{q}, \mathbf{k} - \mathbf{q}) \theta(\mathbf{q}, \tau) \theta(\mathbf{k} - \mathbf{q}, \tau), \end{aligned} \quad (2.2)$$

with

$$\alpha(\mathbf{p}, \mathbf{q}) = \frac{(\mathbf{p} + \mathbf{q}) \cdot \mathbf{p}}{p^2}, \quad \beta(\mathbf{p}, \mathbf{q}) = \frac{(\mathbf{p} + \mathbf{q})^2 \mathbf{p} \cdot \mathbf{q}}{2p^2 q^2}. \quad (2.3)$$

The first equation (2.1) is the continuity equation, while the second equation (2.2) is the Euler equation with the Poisson equation. In the linear regime, one can neglect the mode-coupling terms in the right-hand sides of these equations (2.1) and (2.2). Then the linear solutions are

$$\delta_1(\mathbf{k}, a) = D_1(a) \delta_1(\mathbf{k}), \quad \theta_1(\mathbf{k}, a) = -a^2 H(a) \frac{dD_1(a)}{da} \delta_1(\mathbf{k}), \quad (2.4)$$

The linear growth factor  $D_1(a)$  is determined by

$$\frac{d}{d^2 \ln a^2} \frac{D_1}{a} + \left( 4 + \frac{d \ln H}{d \ln a} \right) \frac{d}{d \ln a} \frac{D_1}{a} + \left( 3 + \frac{d \ln H}{d \ln a} - \frac{3}{2} \Omega_M(a) \right) \frac{D_1}{a} = 0. \quad (2.5)$$

with the initial condition of  $D_1(a)/a \rightarrow 1$  at  $a \rightarrow 0$ . In the special case of the flat model ( $\Omega_K = 0$ ) with the constant  $w$ , the solution is given by the hypergeometric function.<sup>37), 38)</sup>

The density fields are formally expanded up to the third order as  $\delta(\mathbf{k}, a) = \delta_1(\mathbf{k}, a) + \delta_2(\mathbf{k}, a) + \delta_3(\mathbf{k}, a)$ . We will show the second- and third-order solutions in the following sections.

## §3. Second-order solution

Inserting the linear-order solutions of  $\delta_1$  and  $\theta_1$  into the right-hand side of the equations (2.1) and (2.2), one can obtain the second-order solution as,

$$\delta_2(\mathbf{k}, a) = D_{2A}(a) A(\mathbf{k}) + D_{2B}(a) B(\mathbf{k}), \quad (3.1)$$

with

$$A(\mathbf{k}) = \frac{5}{7} \int d^3 \mathbf{q} \alpha(\mathbf{q}, \mathbf{k} - \mathbf{q}) \delta_1(\mathbf{q}) \delta_1(\mathbf{k} - \mathbf{q}), \quad (3.2)$$

$$B(\mathbf{k}) = \frac{2}{7} \int d^3 \mathbf{q} \beta(\mathbf{q}, \mathbf{k} - \mathbf{q}) \delta_1(\mathbf{q}) \delta_1(\mathbf{k} - \mathbf{q}). \quad (3.3)$$

The second-order growth factors  $D_{2A,B}$  are determined by the ordinary differential equations with the boundary condition of  $D_{2A,B} \rightarrow a^2$  at  $a \rightarrow 0$  (see Appendix A). One usually approximately use  $D_1^2$ , instead of  $D_{2A,B}$ , in equation (3.1). In order to demonstrate the validity of this approximation, we show the relative differences between  $D_{2A,B}$  and  $D_1^2$  in Fig.1 for the constant  $w$  in the flat model ( $\Omega_K = 0$ ). The results are shown by the contour lines in the  $\Omega_M - w$  plane for  $D_{2A}$  (top left panel) and for  $D_{2B}$  (top right panel). As clearly seen in the figures, the relative errors are small, less than 4% for  $0.1 < \Omega_M < 1$  and  $-0.5 < w < -1.5$ . The errors become larger for larger  $w$ . This tenancy suggests for larger  $w$  that the dark energy have been affecting the expansion rate since longer time ago, and hence the large differences between  $D_{2A,B}$  and  $D_1^2$  arise at present.

Fig.2 is the same as Fig.1, but for the time varying equation of state,

$$w(a) = w_0 + w_a a (1 - a). \quad (3.4)$$

The results are shown in the  $w_0 - w_a$  plane with  $\Omega_M = 0.28$  ( $= 1 - \Omega_X$ ). As shown in the figure, for large  $w_a$ , the relative differences become large. This is because that the dark energy term in the hubble expansion  $H^2(a)$ ,  $\Omega_X a^{-3(1+w_0)} \exp[(3/2)w_a(1-a)^2]$ , becomes large for large  $w_a$  in the past ( $a < 1$ ). The relative errors are less than 10% for  $-1.5 < w_0 < -0.5$  and  $w_a < 3$ .

#### §4. Third-order solution

Similarly, the third-order solution consists of six terms,

$$\begin{aligned} \delta_3(\mathbf{k}, a) = & D_{3AA}(a)C_{AA}(\mathbf{k}) + D'_{3AA}(a)C'_{AA}(\mathbf{k}) + D_{3AB}(a)C_{AB}(\mathbf{k}) \\ & + D'_{3AB}(a)C'_{AB}(\mathbf{k}) + D_{3BA}(a)C_{BA}(\mathbf{k}) + D_{3BB}(a)C_{BB}(\mathbf{k}), \end{aligned} \quad (4.1)$$

with

$$C_{AA}(\mathbf{k}) = \frac{7}{18} \int d^3 \mathbf{q} \alpha(\mathbf{q}, \mathbf{k} - \mathbf{q}) \delta_1(\mathbf{q}) A(\mathbf{k} - \mathbf{q}), \quad (4.2)$$

$$C'_{AA}(\mathbf{k}) = \frac{7}{30} \int d^3 \mathbf{q} \alpha(\mathbf{q}, \mathbf{k} - \mathbf{q}) \delta_1(\mathbf{k} - \mathbf{q}) A(\mathbf{q}), \quad (4.3)$$

$$C_{AB}(\mathbf{k}) = \frac{7}{18} \int d^3 \mathbf{q} \alpha(\mathbf{q}, \mathbf{k} - \mathbf{q}) \delta_1(\mathbf{q}) B(\mathbf{k} - \mathbf{q}), \quad (4.4)$$

$$C'_{AB}(\mathbf{k}) = \frac{7}{9} \int d^3 \mathbf{q} \alpha(\mathbf{q}, \mathbf{k} - \mathbf{q}) \delta_1(\mathbf{k} - \mathbf{q}) B(\mathbf{q}), \quad (4.5)$$

$$C_{BA}(\mathbf{k}) = \frac{2}{15} \int d^3 \mathbf{q} \beta(\mathbf{q}, \mathbf{k} - \mathbf{q}) \delta_1(\mathbf{q}) A(\mathbf{k} - \mathbf{q}), \quad (4.6)$$

$$C_{BB}(\mathbf{k}) = \frac{4}{9} \int d^3 \mathbf{q} \beta(\mathbf{q}, \mathbf{k} - \mathbf{q}) \delta_1(\mathbf{q}) B(\mathbf{k} - \mathbf{q}). \quad (4.7)$$

There are two additional conditions of

$$\begin{aligned} \frac{5}{18}D_{3AA} + \frac{2}{9}D'_{3AB} &= \frac{1}{2}D_1^3, \\ \frac{1}{6}D'_{3AA} + \frac{1}{9}D_{3AB} + \frac{2}{21}D_{3BA} + \frac{8}{63}D_{3BB} &= \frac{1}{2}D_1^3, \end{aligned} \quad (4.8)$$

and hence only four terms in Eq.(4.1) are independent of each other. The growth factors  $D_{3**}$  are determined by the ordinary differential equations with the boundary conditions of  $D_{3**} \rightarrow a^3$  in  $a \rightarrow 0$  (see Appendix A). The middle and bottom panels in Figs.1 and 2 are same as the top panels, but for the relative differences between  $D_{3**}$  and  $D_1^3$ . The results are shown for  $D_{3AA}$  (middle left),  $D_{3AB}$  (middle right),  $D_{3BA}$  (bottom left), and  $D_{3BB}$  (bottom right). The relative differences are less than 7% for  $0.1 < \Omega_M < 1$  and  $-1.5 < w < -0.5$  and less than 20% for  $-0.5 < w_0 < 0.5$  and  $w_a < 3$ .

Our results of the second- and third-order solutions are consistent with the previous results in Bernardeau (1994) for the cosmological constant model ( $w = -1$ ). While we presented the results only for the density perturbations, one can easily obtain the velocity field perturbations by inserting equations (3.1) and (4.1) to equations (2.1) and (2.2).

## §5. One-Loop Power Spectrum

The one-loop power spectrum is the linear power spectrum with the leading correction arising from the second- and third-order density perturbations,

$$\begin{aligned} P(k, a) &= \left\langle |\delta_1(k, a) + \delta_2(k, a) + \delta_3(k, a)|^2 \right\rangle \\ &= D_1^2(a)P_{11}(k) + P_{22}(k, a) + P_{13}(k, a), \end{aligned} \quad (5.1)$$

where  $P_{11} = \langle |\delta_1|^2 \rangle$ ,  $P_{22} = \langle |\delta_2|^2 \rangle$  and  $P_{13} = \langle 2\text{Re}(\delta_1\delta_3^*) \rangle$ . The first term is the linear power spectrum, the second and third terms are the one-loop corrections. The explicit formulae for  $P_{22}$  and  $P_{13}$  are given in Appendix B.

One usually approximately apply the one-loop power spectrum in the EdS model to an arbitrary cosmological model by replacing the scale factor by the linear growth factor,

$$P_{\text{EdS}}(k, a) = D_1^2(a)P_{11}(k) + D_1^4(a)[P_{22}(k) + P_{13}(k)]_{\text{EdS}}. \quad (5.2)$$

where the second and third terms are the corrections for the EdS model<sup>27),28)</sup> (see also Appendix B). We compare the two power spectra in Eqs.(5.1) and (5.2) in order to demonstrate quantitatively the validity of the above approximation. We use CAMB (Code for Anisotropies in the Microwave Background)<sup>40)</sup> to calculate the linear power spectrum with the cosmological parameters of  $h = 0.701$ ,  $\Omega_B = 0.0462$ ,  $\Omega_M = 0.279$ ,  $n_s = 0.96$ , and  $\sigma_8 = 0.82$ , consistent with the WMAP 5yr result.<sup>39)</sup>

Fig.3 shows the relative differences of  $P_{22}(k)$ ,  $P_{13}(k)$ ,  $P_{22}(k) + P_{13}(k)$  and  $P(k)$  between equations (5.1) and (5.2) at  $z = 0$ . The equation of states are  $(w_0, w_a) = (-1.2, 0)$ ,  $(-1, 0)$ ,  $(-1, 2)$ , and  $(-0.8, 0)$ . From top panels, the error is  $< 5\%$  for  $P_{13}$  while  $\ll 1\%$  for  $P_{22}$ . For small scale, these differences become small. In bottom left

panel, the error diverges at  $k \simeq 0.75h/\text{Mpc}$  because the denominator of  $P_{22} + P_{13}$  vanishes there. The approximate formula of  $P_{\text{EdS}}$  predicts slightly less value than the correct result, because that  $[P_{22}]_{\text{EdS}} (> 0)$  is almost same while  $[P_{13}]_{\text{EdS}} (< 0)$  is more negative as shown in top panels. However, as expected, the difference is very small less than  $\sim 1\%$  for  $k < 0.4h/\text{Mpc}$ . Fig.4 is the same as Fig.3, but at the various redshifts of  $z = 0, 1, 3$ . Hence, from this figure, the EdS model approximation in Eq.(5.2) is sufficiently more accurate for higher redshift  $z > 1$ .

Finally we calculate the shift of the position of the first acoustic peak at  $k \simeq 0.07h/\text{Mpc}$ . Dividing  $P(k)$  by the no-wiggle model of Eisenstein & Hu (1999), we find that the position is shifted by only  $0.8\%$  ( $0.02\%$ ) for  $z = 0$  ( $z = 1$ ).

In this chapter, we have calculated the one-loop power spectrum, however it is not accurate in the strong non-linear regime ( $k \gtrsim 0.1h/\text{Mpc}$ ). In fact, Jeong & Komatsu (2006) found that the one-loop power spectrum coincides with the non-linear power spectrum from the numerical simulation within  $1\%$  if  $\Delta^2(k) = k^3 P(k)/2\pi^2 < 0.4$  is satisfied. This condition is rewritten as  $k < 0.12(0.26)h/\text{Mpc}$  at  $z = 0$  ( $z = 1$ ). Hence in order to extend our analysis to smaller scale, the further analysis for investigating the cosmological dependence of the higher order perturbation theory is necessary.

## §6. Conclusion

We investigate the third-order density perturbation and the one-loop power spectrum in the dark energy cosmological model. We present the analytical solutions and the fitting formula with the general time varying equation of state for the first time. It turns out that the cosmological dependence is very weak, for example, less than  $1\%$  for  $k < 0.4h/\text{Mpc}$  for the power spectrum. However, our results may be useful in some cases when one needs very high accurate model of the BAO or study the non-linear evolution at the smaller scale ( $> 0.4h/\text{Mpc}$ ).

## Acknowledgements

We would like to thank Takahiko Matsubara and the anonymous referees for useful comments and suggestions. This work is supported in part by Grant-in-Aid for Scientific Research on Priority Areas No. 467 ‘‘Probing the Dark Energy through an Extremely Wide and Deep Survey with Subaru Telescope’’.

## Appendix A

### — Second and Third Order Growth Factors —

The second-order growth factors  $D_{2A,B}$  are determined by the following ordinary differential equations,

$$\frac{d^2}{d \ln a^2} \frac{D_2}{a^2} + \left( 6 + \frac{d \ln H}{d \ln a} \right) \frac{d}{d \ln a} \frac{D_2}{a^2} + \left[ 8 + 2 \frac{d \ln H}{d \ln a} - \frac{3}{2} \Omega_M(a) \right] \frac{D_2}{a^2}$$

$$= \frac{7}{5} \left[ \left( \frac{dD_1}{da} \right)^2 + \frac{3}{2} \Omega_M(a) \left( \frac{D_1}{a} \right)^2 \right] \text{ for } D_{2A}, \quad (\text{A}\cdot 1)$$

$$= \frac{7}{2} \left( \frac{dD_1}{da} \right)^2 \text{ for } D_{2B}, \quad (\text{A}\cdot 2)$$

with the initial conditions at  $a = 0$  :

$$\frac{D_{2A,B}}{a^2} = 1, \quad \frac{d}{da} \frac{D_{2A,B}}{a^2} = 0. \quad (\text{A}\cdot 3)$$

For the flat model with the constant equation of state, the solutions are well approximated as,

$$D_{2A} \simeq D_1^2 \left[ 1 + |\ln \Omega_M| \left( \frac{5.54 \times 10^{-3}}{|w|} - \frac{3.40 \times 10^{-3}}{\sqrt{|w|}} \right) \right], \quad (\text{A}\cdot 4)$$

$$D_{2B} \simeq D_1^2 \left[ 1 + |\ln \Omega_M| \left( -\frac{1.384 \times 10^{-2}}{|w|} + \frac{8.50 \times 10^{-3}}{\sqrt{|w|}} \right) \right], \quad (\text{A}\cdot 5)$$

within maximum error of 0.03% for both  $0.1 \leq \Omega_M \leq 1$  and  $-1.5 \leq w \leq -0.5$ .

Similarly, the third-order growth factors are determined by the following equations,

$$\begin{aligned} & \frac{d^2}{d \ln a^2} \frac{D_3}{a^3} + \left( 8 + \frac{d \ln H}{d \ln a} \right) \frac{d}{d \ln a} \frac{D_3}{a^3} + \left[ 15 + 3 \frac{d \ln H}{d \ln a} - \frac{3}{2} \Omega_M(a) \right] \frac{D_3}{a^3} \\ &= \frac{18}{7} \left[ 2 \frac{dD_1}{da} + \frac{3}{2} \Omega_M(a) \frac{D_1}{a} \right] \frac{D_{2A,B}}{a^2} + \frac{18}{7} a \frac{dD_1}{da} \frac{d}{da} \frac{D_{2A,B}}{a^2} \text{ for } D_{3AA,3AB} \end{aligned} \quad (\text{A}\cdot 6)$$

$$= 15 \frac{dD_1}{da} \left[ a \frac{d}{da} \frac{D_{2A}}{a^2} + 2 \frac{D_{2A}}{a^2} - \frac{7}{5} \frac{D_1}{a} \frac{dD_1}{da} \right], \text{ for } D_{3BA} \quad (\text{A}\cdot 7)$$

$$= \frac{9}{2} \frac{dD_1}{da} \left[ a \frac{d}{da} \frac{D_{2B}}{a^2} + 2 \frac{D_{2B}}{a^2} \right], \text{ for } D_{3BB} \quad (\text{A}\cdot 8)$$

with the initial conditions at  $a = 0$  :

$$\frac{D_3}{a^3} = 1, \quad \frac{d}{da} \frac{D_3}{a^3} = 0. \quad (\text{A}\cdot 9)$$

For  $\Omega_K = 0$  with the constant  $w$ , the solutions are well fitted by,

$$D_{3AA} \simeq D_1^3 \left[ 1 + |\ln \Omega_M| \left( \frac{8.21 \times 10^{-3}}{|w|} - \frac{5.14 \times 10^{-3}}{\sqrt{|w|}} \right) \right], \quad (\text{A}\cdot 10)$$

$$D_{3AB} \simeq D_1^3 \left[ 1 + |\ln \Omega_M|^{1.5+0.4 \ln |w|} |\Omega_M|^{0.7|w|} \left( -\frac{9.16 \times 10^{-3}}{|w|} + \frac{8.95 \times 10^{-3}}{\sqrt{|w|}} \right) \right],$$

$$D_{3BA} \simeq D_1^3 \left[ 1 + |\ln \Omega_M|^{1.06-0.5 \ln |w|} \left( 7.68 \times 10^{-3} |w| - 1.130 \times 10^{-2} \sqrt{|w|} \right) \right] \quad (\text{A}\cdot 11)$$

$$D_{3BB} \simeq D_1^3 \left[ 1 + |\ln \Omega_M| \left( -\frac{2.641 \times 10^{-2}}{|w|} + \frac{1.582 \times 10^{-2}}{\sqrt{|w|}} \right) \right], \quad (\text{A}\cdot 13)$$

within maximum error of 0.05% for both  $0.1 \leq \Omega_M \leq 1$  and  $-1.5 \leq w \leq -0.5$ . The other growth factors of  $D'_{3AA}$  and  $D'_{3AB}$  can be obtained from Eq.(4.8).

## Appendix B

### — Explicit Expressions for $P_{22}$ and $P_{13}$ —

Here we present the explicit expressions for the one-loop correction terms  $P_{22}$  and  $P_{13}$ . From the results in §3, we obtain

$$P_{22}(k, a) = \langle |\delta_2(\mathbf{k}, a)|^2 \rangle = D_{2A}^2(a)P_{2AA}(k) + 2D_{2A}(a)D_{2B}(a)P_{2AB}(k) + D_{2B}^2(a)P_{2BB}(k), \quad (\text{B}\cdot 1)$$

with

$$P_{2AA}(k) = \frac{25}{392\pi^2} k^4 \int_0^\infty dk_1 \int_{-1}^1 d\mu P_{11}(k_1) P_{11} \left( \sqrt{k^2 + k_1^2 - 2kk_1\mu} \right) \left( \frac{k\mu + k_1 - 2k_1\mu^2}{k^2 + k_1^2 - 2kk_1\mu} \right)^2,$$

$$P_{2BB}(k) = \frac{1}{98\pi^2} k^4 \int_0^\infty dk_1 \int_{-1}^1 d\mu P_{11}(k_1) P_{11} \left( \sqrt{k^2 + k_1^2 - 2kk_1\mu} \right) \left( \frac{k\mu - k_1}{k^2 + k_1^2 - 2kk_1\mu} \right)^2,$$

$$P_{2AB}(k) = \frac{5}{196\pi^2} k^4 \int_0^\infty dk_1 \int_{-1}^1 d\mu P_{11}(k_1) P_{11} \left( \sqrt{k^2 + k_1^2 - 2kk_1\mu} \right) \frac{(k\mu - k_1)(k\mu + k_1 - 2k_1\mu^2)}{(k^2 + k_1^2 - 2kk_1\mu)^2},$$

where  $\mu$  is the cosine between  $\mathbf{k}$  and  $\mathbf{k}_1$ .

Similarly for  $P_{13}$ , from the results in §4, we obtain

$$P_{13}(k, a) = \langle 2\text{Re}(\delta_1(\mathbf{k}, a)\delta_3^*(\mathbf{k}, a)) \rangle$$

$$= D_{3AA}(a)P_{3AA}(k) + D'_{3AA}(a)P'_{3AA}(k) + D_{3AB}(a)P_{3AB}(k)$$

$$+ D'_{3AB}(a)P'_{3AB}(k) + D_{3BA}(a)P_{3BA}(k) + P_{3BB}(a)P_{3BB}(k), \quad (\text{B}\cdot 2)$$

with

$$P_{3AA}(k) = -\frac{5}{54\pi^2} k^3 P_{11}(k) \int_0^\infty dr P_{11}(kr) (1 + r^2),$$

$$P'_{3AA}(k) = \frac{1}{24\pi^2} k^3 P_{11}(k) \int_0^\infty dr P_{11}(kr) \left[ 1 + 4r^2 - r^4 + \frac{1}{2r} (r^2 - 1)^3 \ln \left| \frac{r+1}{r-1} \right| \right],$$

$$P_{3AB}(k) = -\frac{1}{27\pi^2} k^3 P_{11}(k) \int_0^\infty dr P_{11}(kr) (1 + r^2),$$

$$P'_{3AB}(k) = \frac{2}{27\pi^2} k^3 P_{11}(k) \int_0^\infty dr P_{11}(kr) r^2,$$

$$P_{3BA}(k) = \frac{1}{168\pi^2} k^3 P_{11}(k) \int_0^\infty dr P_{11}(kr) \left[ \frac{2}{r^2} (1 - 4r^2 - r^4) + \frac{(r^2 - 1)^3}{r^3} \ln \left| \frac{r+1}{r-1} \right| \right],$$

$$P_{3BB}(k) = -\frac{4}{189\pi^2} k^3 P_{11}(k) \int_0^\infty dr P_{11}(kr).$$

By setting  $D_2 = a^2$  and  $D_3 = a^3$  in equations (B·1) and (B·2), the correction terms reduce to the result in the EdS model,  $a^4[P_{22}(k) + P_{13}(k)]_{\text{EdS}}$ .

### References

- 1) D.J. Eisenstein, et al., *Astrophys. J.*, **633** (2005), 560
- 2) S. Cole, et al., *Mon. Not. R. Astron. Soc.*, **362** (2005), 505
- 3) W.J. Percival, et al., *Mon. Not. R. Astron. Soc.*, **381** (2007), 1053
- 4) T. Okumura, et al., *Astrophys. J.*, **676** (2008), 889
- 5) H.J. Seo & D.J. Eisenstein, *Astrophys. J.*, **633** (2005), 575
- 6) R.E. Angulo, C.M. Baugh, C.S. Frenk, & C.G. Lacey, *Mon. Not. R. Astron. Soc.*, **383** (2008), 755.
- 7) E. Huff, et al., *Astroparticle Physics* **26** (2007), 351
- 8) R.E. Smith, R. Scoccimarro, & R.K. Sheth, *Phys. Rev. D*, **75** (2007), 063512
- 9) R.E. Smith, R. Scoccimarro, & R.K. Sheth, *Phys. Rev. D*, **77** (2008), 043525
- 10) R. Takahashi, et al., submitted to *Mon. Not. R. Astron. Soc.*, (2008), arXiv:0802.1808
- 11) A.G. Sanchez, C.M. Baugh, & R. Angulo, submitted to *Mon. Not. R. Astron. Soc.*, (2008), arXiv:0804.0233
- 12) H.-J. Seo, E.R. Siegel, D.J. Eisenstein, & M. White, submitted to *Astrophys. J.*, (2008), arXiv:0805.0117
- 13) D. Jeong & E. Komatsu, *Astrophys. J.*, **651** (2006), 619
- 14) M. Crocce & R. Scoccimarro, *Phys. Rev. D*, **77** (2008), 023533
- 15) M. Crocce & R. Scoccimarro, *Phys. Rev. D*, **73** (2006), 063519
- 16) T. Matsubara, *Phys. Rev. D*, **77** (2008), 063530
- 17) P. McDonald, *Phys. Rev. D*, **75**, (2007), 043514
- 18) A. Taruya & T. Hiramatsu, *Astrophys. J.*, **674** (2008), 617.
- 19) K. Izumi & J. Soda, *Phys. Rev. D*, **76** (2007), 083517.
- 20) S. Matarrese & M. Pietroni, *JCAP*, **06** (2007), 026.
- 21) T. Nishimichi et al., *PASJ*, **59** (2007), 1049.
- 22) D. Jeong & E. Komatsu, (2008), arXiv:0805.2632
- 23) R. Juszkiewicz, *Mon. Not. R. Astron. Soc.*, **197** (1981), 931
- 24) E.T. Vishniac, *Mon. Not. R. Astron. Soc.*, **203** (1983), 345
- 25) M.H. Goroff, B. Grinstein, S.J. Rey, & M.B. Wise, *Astrophys. J.*, **311** (1986), 1.
- 26) Y. Suto & M. Sasaki, *Phys. Rev. Lett.*, **21** (1991), 264.
- 27) N. Makino, M. Sasaki & Y. Suto, *Phys. Rev. D*, **46** (1992), 585.
- 28) B. Jain & E. Bertschinger, *Astrophys. J.*, **431** (1994), 495.
- 29) H. Martel & W. Freudling, *Astrophys. J.*, **371** (1991), 1.
- 30) R. Scoccimarro, et al., *Astrophys. J.*, **496** (1998), 586.
- 31) F. Bernardeau, S. Colombi, E. Gaztanaga, & R. Scoccimarro, *Phys. Rep.*, **367** (2002), 1.
- 32) F.R. Bouchet, R. Juszkiewicz, S. Colombi, & R. Pellat, *Astrophys. J.*, **394** (1992), L5.
- 33) F. Bernardeau, *Astrophys. J.*, **433** (1994), 1.
- 34) F.R. Bouchet, S. Colombi, E. Hivon, & R. Juszkiewicz, *Astron. Astrophys.*, **296** (1995), 575.
- 35) P. Catelan, F. Lucchin, S. Matarrese, & L. Moscardini, *Mon. Not. R. Astron. Soc.*, **276** (1995), 39.
- 36) T. Matsubara, *Prog. Theor. Phys.*, **94** (1995), 1151
- 37) V. Silveira & I. Waga, *Phys. Rev. D*, **50** (1994), 4890.
- 38) T. Padmanabhan, *Phys. Rep.*, **380** (2003), 235
- 39) E. Komatsu et al., submitted to *Astrophys. J. Suppl.*, arXiv:0803.054, (2008)
- 40) A. Lewis, A. Challinor, & A. Lasenby, *Astrophys. J.*, **538** (2000), 473.
- 41) D.J. Eisenstein & W. Hu, *Astrophys. J.*, **511** (1999), 5.



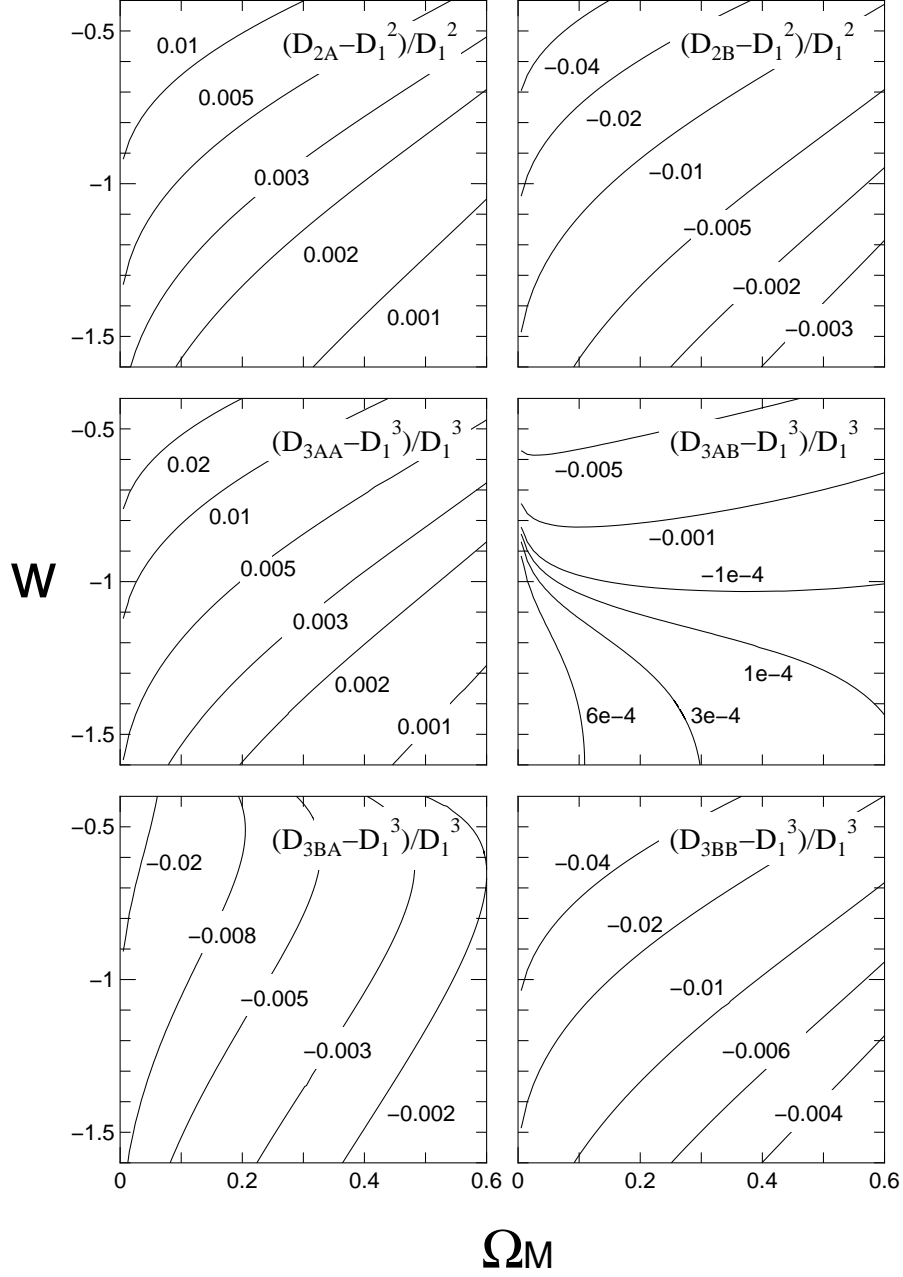


Fig. 1. Top panels : the contour lines show the relative differences between  $D_{2A,B}$  and  $D_1^2$  at present ( $a = 1$ ) in the  $\Omega_M - w$  plane. The flat cosmological model and the constant equation of state are assumed. The top left (right) panel is the result for  $D_{2A}$  ( $D_{2B}$ ). Middle and Bottom panels : same as top panels, but for the relative differences between  $D_3$  and  $D_1^3$ .

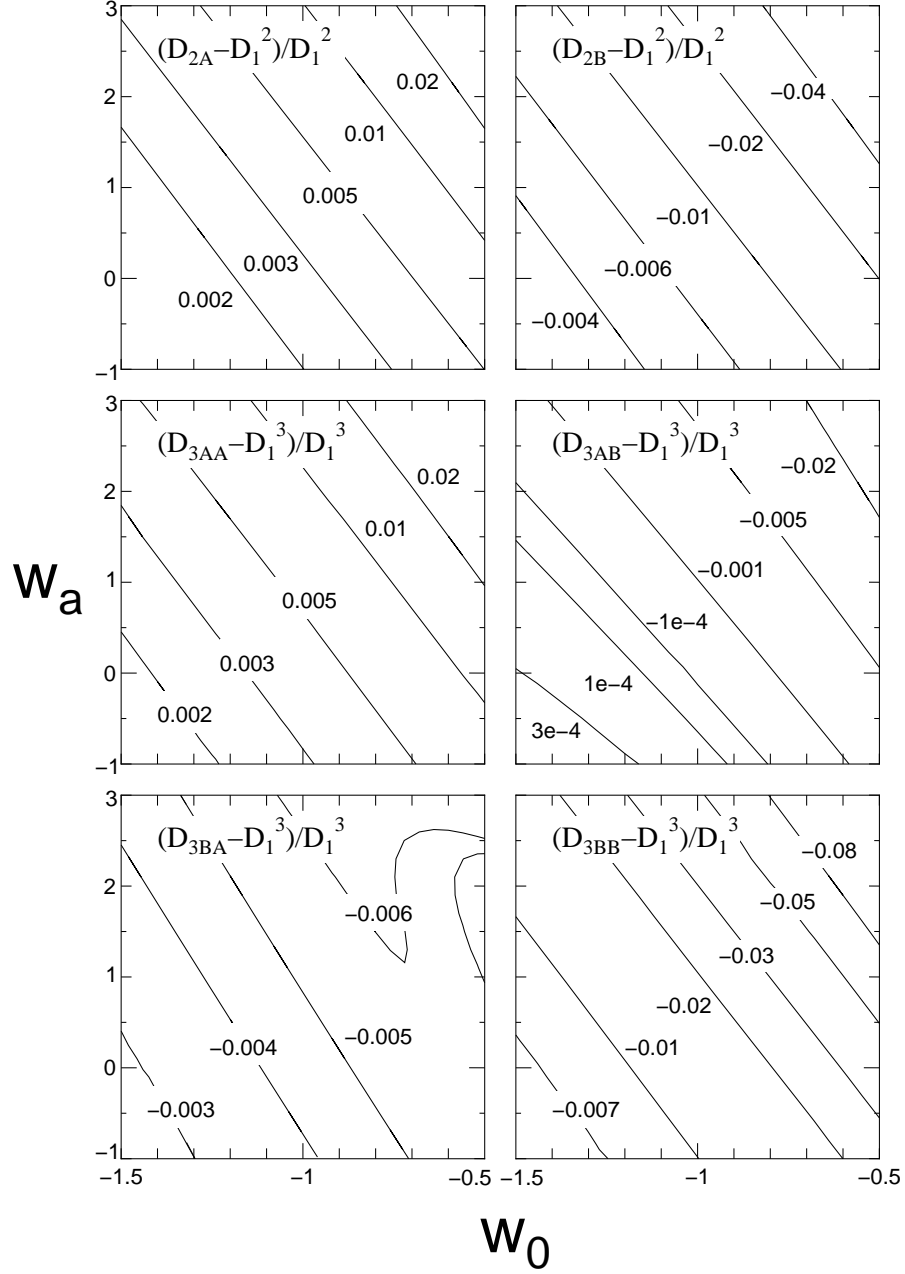


Fig. 2. Same as Fig.1, but for the time varying equation of state,  $w(a) = w_0 + w_a a(1 - a)$ . The results are shown in the  $w_0 - w_a$  plane in the flat cosmological model with  $\Omega_M = 0.28$ .

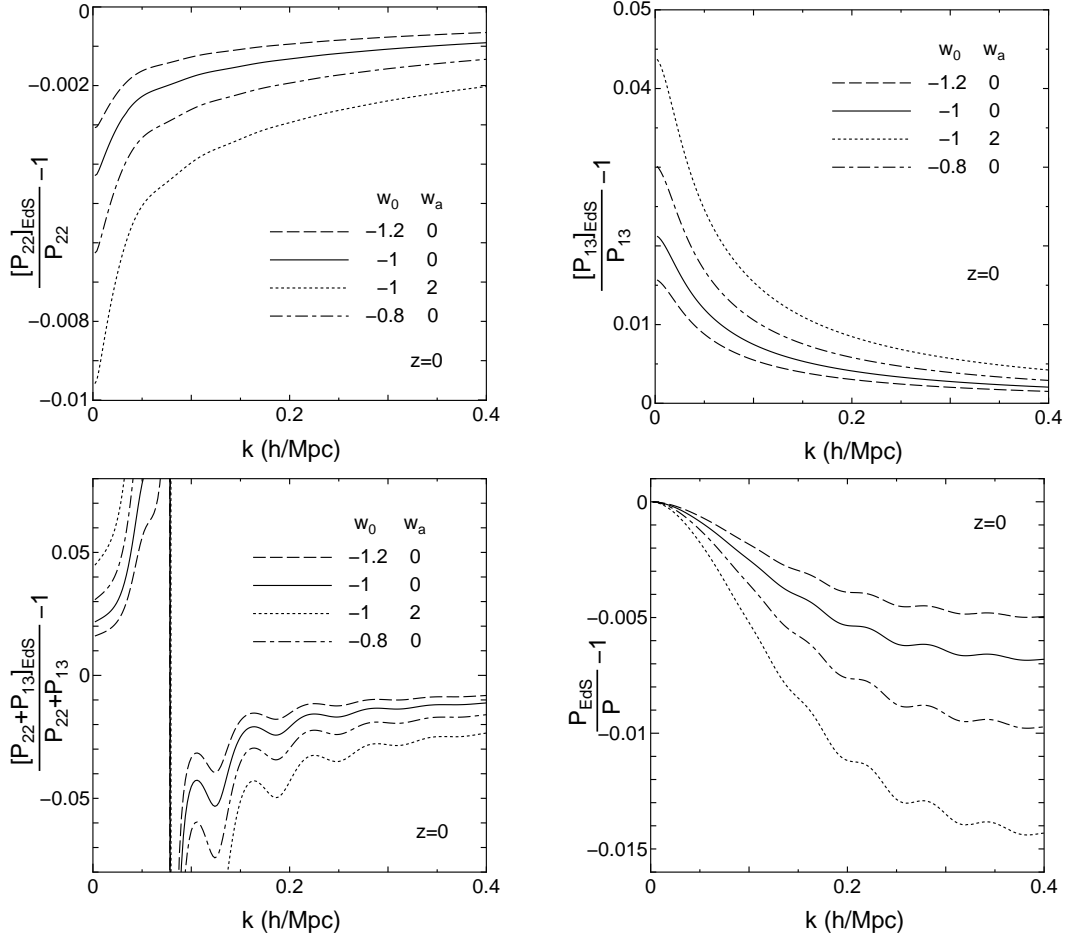


Fig. 3. The relative differences of  $P_{22}(k)$  (top left),  $P_{13}(k)$  (top right),  $P_{22}(k) + P_{13}(k)$  (bottom left) and  $P(k)$  (bottom right) between the correct results and the approximate results denoted by  $[\dots]_{\text{EdS}}$ . The cosmological model is consistent with WMAP 5yr result.

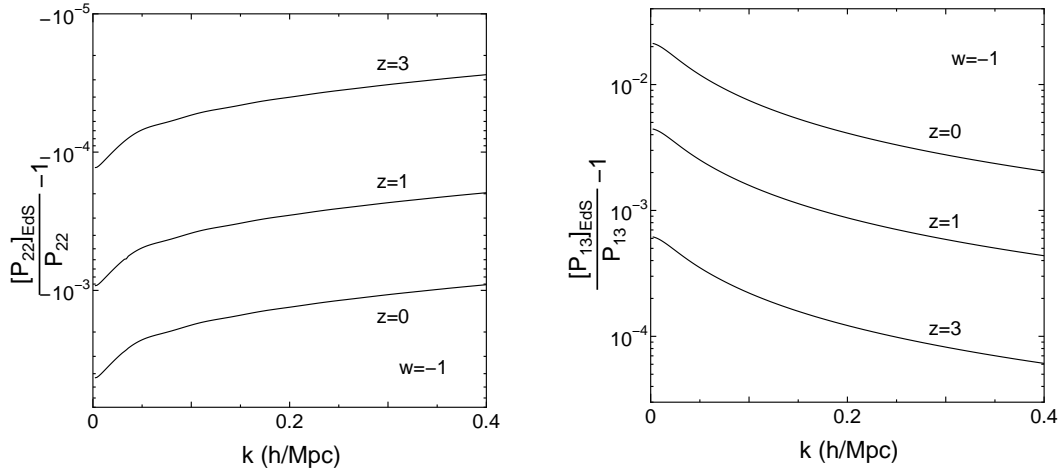


Fig. 4. Same as top panels of Fig.3, but at the various redshifts of  $z = 0, 1, 3$ .